Numerical investigation on convergence of boundary knot method in the analysis of homogeneous Helmholtz, modified Helmholtz, and convection-diffusion problems

W. Chen*

Simula Research Laboratory, P. O. Box. 134, NO-1325 Lysaker, Norway

Y. C. Hon

Department of Mathematics, City University of Hong Kong, Hong Kong SAR, China

Abstract

This paper concerns a numerical study of convergence properties of the boundary knot method (BKM) applied to the solution of 2D and 3D homogeneous Helmholtz, modified Helmholtz, and convection-diffusion problems. The BKM is a new boundary-type, meshfree radial function basis collocation technique. The method differentiates from the method of fundamental solutions (MFS) in that it does not need the controversial artificial boundary outside physical domain due to the use of non-singular general solutions instead of the singular fundamental solutions. The BKM is also generally applicable to a variety of inhomogeneous problems [11,12,22] in conjunction with the dual reciprocity method (DRM). Therefore, when applied to inhomogeneous problems, the error of the DRM confounds the BKM accuracy in approximation of homogeneous solution, while the latter essentially distinguishes the BKM, MFS, and boundary element method. In order to avoid the interference of the DRM, this study focuses on the investigation of the convergence property of the BKM for homogeneous problems. The given numerical experiments reveal rapid convergence, high accuracy and efficiency, mathematical simplicity of the BKM.

Keywords: boundary knot method, radial basis function, method of fundamental solution, meshfree, boundary elements.

* Corresponding author, email: wenc@simula.no

.

1. Introduction

Due to the pioneer work by Nardini and Brebbia [1], the boundary element method in conjunction with dual reciprocity method (DRM) and radial basis function (RBF), can now be used to obtain approximate solutions of general partial differential equation (PDE) systems. This strategy is often called as the dual reciprocity BEM (DR-BEM) [2]. An explosive increase in applying the DR-BEM to various problems is seen in recent years [3]. However, as was pointed out by Golberg and Chen [4], the DR-BEM still suffers some inefficiencies inherent in the standard BEMs. Compared with the FEM, the method is mathematically more complicated to learn and to use for common engineers. Handling singular integral is also often cumbersome and the lower order of polynomial approximation greatly slows its convergence speed. For higher-dimensional moving boundary and discontinuous problems, the mesh or remesh can be very time-consuming. As a consequence, the method of fundamental solution (MFS), originally introduced in Russian in 1964 [5], was strongly recommended by ref. [4,6]. The method is also called as the regular BEM in some literature [7]. The MFS is indeed simple to learn and to program and has spectral convergence and high order of accuracy. More importantly, the MFS combining with the DRM and RBF is an essentially meshfree technique for various higher-dimensional PDEs, which is especially attractive in handling moving boundary, nonlinear and multiscale problems [4,8]. Despite these salient merits, the MFS has not been popular in the computational engineering community [9]. The blame goes to the controversial artificial boundary outside physical domain [7] to circumvent the singularity of the fundamental solutions. An arbitrary in determining the fictitious boundary significantly downgrades the practical applicability of the method, especially for complicated-shape problems [7,10].

As an alternative technique, Chen and Tanaka [11,12] introduced the boundary knot method, which eliminates the drawback applying the ambiguous auxiliary boundary and holds all advantages of the MFS. The essential difference between the BKM and MFS is that the former uses the non-singular general solutions instead of the singular fundamental solutions. With the help of the DRM and RBF, the BKM was also tested successfully in some inhomogeneous problems [11,12]. The method is a truly meshfree, integration-free, mathematically simple, boundary-type, RBF collocation

discretization technique for a variety of PDE systems. Unlike the other meshfree FEM and BEM schemes based on moving least squares [13], the RBF-based schemes requires no mesh either for interpolating variables or for numerical integrations in handling high-dimensional problems with any complex-shaped domains. This inherent meshfree advantage in the BKM owes to the fact that the method is a pure radial basis function technique.

Very recently, the authors became aware of relevant pioneer works by Kang et al [14-16] and Chen et al [17-20], where the nonsingular general solutions, the influence functions called in Kang et al [14-16], of the Helmholtz equation and thin plate vibration equation are first employed to construct a meshfree boundary-only collocation formulation of the corresponding eigenvalue problems. Their approach is closely similar to the BKM in that both use the nonsingular general solution to evaluate the homogeneous solution. As mentioned by Chen et al [17], the nonsingular general solution of the Helmholtz equation has also in fact earlier been used by DE MEY [21] with a weak form boundary integral formulation to evaluate the Helmholtz eigenvalue problems. It is noted that different from the approach given in [14-20], the BKM is feasible for the inhomogeneous and nonlinear problems in general in conjunction with the dual reciprocity method for the evaluation of the particular solution. A symmetric nonsingular boundary formulation was also proposed in Chen [22] for dealing with self-adjoint problems having mixed boundary conditions.

The RBF was originally introduced in the early 1970s to multivariate scattered data approximation and function interpolation [23]. The strategy has since been applied to neural network, computational geometry [24,25], and most recently, numerical PDEs [1,26]. The prominent merits of the RBF approaches are independent of dimensionality and geometric complexity, and mathematically very simple to implement [27-30]. For example, the introducing the RBF into the BEM [1] has eliminated its major weakness in handling general inhomogeneous terms, while the domain-type RBF collocation method, pioneered by Kansa [26], is very promising for a wide range of problems. Nevertheless, constructing efficient RBF is still an open research topic. Chen and Tanaka [31] attributed the prowess of the RBF to the essential relationship between Euclidean distance concept and the field theory, and more broadly, to kernel functions of convolution integral equations. A general strategy

creating efficient operator-dependent kernel RBF was also presented there on the grounds of integral equation theory, in particular, the Green second identity for numerical PDE.

As a boundary-type RBF methodology, the BKM has great potential to handle a broad range of problems. The method has been applied successfully to 2D linear homogeneous and inhomogeneous Dirichlet Helmholtz, modified Helmholtz, and nonlinear Burger problems with a smooth elliptical domain [11,12,31,32]. Hon and Chen [33] also verified that for Helmholtz and convection-diffusion problems having 2D domain with sharp outside corners and inside cutouts and mixed Dirichlet and Neumann boundary conditions, the BKM produced very accurate, stable solutions with small numbers of nodes. Due to its very recent origin, however, the systematic numerical and theoretical studies on the issues of convergence, stability, and accuracy are still missing now. As was mentioned earlier, the DRM and RBF are employed in the BKM to approximate the particular solution of inhomogeneous problems. Therefore, in terms of resulting experimental results, the error of the DRM confounds the BKM accuracy in approximation of homogeneous solution, while the latter essentially distinguishes the BKM, MFS, and boundary element method. It is well known that the accuracy of the DRM approximation is largely dependent on the proper choice of the RBF just as used in the MFS and DR-BEM. An in-depth analysis of this issue is beyond the present study. The readers are advised to see an excellent analysis of the DRM convergence and accuracy given in [34]. For the BKM solution of inhomogeneous problems see refs. [11,12,31-33]. In order to avoid the interference of the DRM, this paper focuses on numerical investigation of convergence, stability, and accuracy of the BKM in the analysis of some typical 2D and 3D homogeneous Helmholtz, modified Helmholtz, and convection-diffusion problems.

In what follows, the BKM is introduced first in section 2, followed by numerical investigation of convergence, accuracy, and stability in section 3, and finally, some remarks are presented based on the results reported herein.

2. Boundary knot method and applications

The BKM divides the solution of the general PDEs into two components of homogeneous and particular solutions. Like the MFS and DR-BEM, the DRM and RBF are usually used to evaluate the particular solution, and then, differently from both, the BKM formulates the resulting homogeneous solutions in terms of the non-singular general solutions of the respective homogeneous equation. The DRM has been well developed in recent years [2,4,34]. For completeness, we briefly present its basic methodology first, and after that, the non-singular general formulation for homogeneous solution is introduced in details.

2.1. Approximation of Particular Solution

Let us consider the modified Hemholtz problem

$$\nabla^2 u - \lambda^2 u = f(x) \tag{1}$$

defined in a region V bounded by a surface S as an illustrative case, where $f(x)$ is inhomogeneous term and x represents multidimensional independent variable. Boundary conditions on surface S are stated in a general form

$$u(x) = R(x), \quad x \subset S_u, \tag{2}$$

$$\frac{\partial u(x)}{\partial n} = N(x), \, x \subset S_T, \tag{3}$$

where n is the unit outward normal. The solution of Eq. (1) can be decomposed as

$$u = u_h + u_p, \tag{4}$$

where u_h and u_p are respectively the homogeneous and particular solutions. The particular solution satisfies

$$\nabla^2 u_p - \lambda^2 u_p = f(x), \tag{5}$$

but does not necessarily satisfy boundary conditions, while the homogeneous solution v satisfies

$$\nabla^2 u_h - \lambda^2 u_h = 0, \tag{6}$$

$$u_h(x) = R(x) - u_p, \tag{7}$$

$$\frac{\partial u_h(x)}{\partial n} = N(x) - \frac{\partial u_p(x)}{\partial n}, \tag{8}$$

To evaluate the particular solution, the left-side inhomogeneous term of Eq. (5) is approximated first by

$$f(x) \cong \sum_{k=1}^{N+L} \alpha_k \phi(r_k), \tag{9}$$

where $r_k = \|x - x_k\|$ represent the Euclidean norm distance; φ is the RBF; and α_k are the unknown coefficients. N and L respectively denote the numbers of knots on boundary and domain. If the RBF φ is conditionally positive definite, a linear polynomial term φ is usually added [4,34-36]. In terms of Eq. (9), we have

$$\alpha = A_\phi^{-1} f(x), \tag{10}$$

where A_φ is the RBF interpolation matrix. Finally, we get particular solutions at any point by summing localized approximate particular solutions

$$u_p = \sum_{k=1}^{N+L} \alpha_k \Phi(r_k), \tag{11}$$

where Φ is related to the radial basis function φ, namely,

$$\nabla^2\Phi - \lambda^2\Phi = \phi\,. \tag{12}$$

In [2,11,12,31,33] the approximate particular solution Φ is determined beforehand, and then we evaluate the corresponding RBF φ by a simple differentiation process, while in [4,34], the RBF φ is a priori defined, and accordingly, the analytical approximate solution Φ is then derived by a sophisticated integration procedure. Both approaches work equally well in practical numerical computations. The latter is, however, practically workable only in the limited cases [4].

2.2. Non-singular general solution formulation

What differentiates the BKM from the DR-BEM and MFS is that the former applies the non-singular general solution to produce a boundary-only formulation of the homogeneous problems. In terms of the homogeneous modified Helmholtz equation [7], the non-singular general solution is given by

$$u_n^{\#}(r) = \frac{1}{2\pi}\left(\frac{\lambda}{2\pi r}\right)^{(n/2)-1} I_{(n/2)-1}(\lambda r), \qquad n\geq 2, \tag{13}$$

and the singular fundamental solution

$$u_n^{*}(r) = \frac{1}{2\pi}\left(\frac{\lambda}{2\pi r}\right)^{(n/2)-1} K_{(n/2)-1}(\lambda r), \quad n\geq 2, \tag{14}$$

where I and K represent the modified Bessel functions of the first and second kinds, respectively. It is noted that K has logarithm singularity at the origin, which leads to troublesome singular integral in the BEM and controversial fictitious boundary in the MFS.

By using the non-singular general solution (13), the homogeneous solution of Eq. (6) is represented by a weighted linear sum of function values of the non-singular solution at all boundary nodes, i.e.,

$$u_h(x) = \sum_{j=1}^{L} \beta_j u_n^{\#}(r_j), \tag{15}$$

where j is index of source points on physical boundary; and L denotes the total number of boundary knots; and β_j are the desired coefficients. Collocating boundary equations (7) and (8) by approximation representation (15), we have

$$\sum_{j=1}^{L_D} \beta_j u_n^{\#}(r_{ij}) = R(x_i) - u_p(x_i), \tag{16}$$

$$\sum_{m=1}^{L_N} \beta_j \frac{\partial u_n^{\#}(r_{mj})}{\partial n} = N(x_m) - \frac{\partial u_p(x_m)}{\partial n}, \tag{17}$$

where i and m indicate boundary response knots respectively located on Dirichlet surface S_u and Neumann surface S_Γ; and L_D and L_N are the corresponding numbers of the response nodes. For the inhomogeneous problems, the following equations at interior knots are supplemented

$$\sum_{j=1}^{N} \beta_j u_n^{\#}(r_{lj}) = u_l - u_p(x_l), \qquad l = 1, \ldots, N, \tag{18}$$

where N is the total number of interior points used. Eqs. (16), (17) and (18) make up of the resulting simultaneous algebraic equations. It is seen from the preceding procedure that unlike the MFS, the BKM places all nodes only on physical boundary and the same set of boundary knots is used as either source or response points.

2.3. Non-singular general solutions of Helmholtz and convection-diffusion operators

It is straightforward to extend the above BKM procedure for the modified Helmholtz problems to more general cases. We here present the non-singular general solutions of Helmholtz and convection-diffusion operators. For the non-singular general solutions of the other known operators such as time-dependent diffusion and wave operators, biharmonic operators see Chen and Tanaka [31]. Note that the following x and r respectively represent n-dimensional independent variable and the corresponding Euclidean distance. For the homogeneous Helmholtz equation

$$\nabla^2 w + \lambda^2 w = 0, \tag{19}$$

the non-singular general solution is

$$w_n^{\#}(r) = \left(\frac{\lambda}{2\pi r}\right)^{n/2-1} J_{n/2-1}(\lambda r),\ n \geq 2, \tag{20}$$

where J is the Bessel function of the first kind. For the convection-diffusion operator

$$D\nabla^2 p + v \bullet \nabla p - kp = 0, \tag{21}$$

where D denotes the diffusivity; k represents the reaction coefficient; $\boldsymbol{v}$ is velocity vector; and marked $\boldsymbol{r}$ denotes the distance vector between the source and response knots. Its non-singular general solution is

$$p_n^{\#}(r) = \frac{1}{2\pi}\left(\frac{\mu}{2\pi r}\right)^{(n/2)-1} e^{-\frac{v \cdot r}{2D}} I_{(n/2)-1}(\mu r), \qquad n \geq 2, \tag{22}$$

where

$$\mu = \left[\left(\frac{|v|}{2D}\right)^2 + \frac{k}{D}\right]^{\frac{1}{2}}. \tag{23}$$

In section 3, we will investigate 2D and 3D homogeneous Helmholtz, modified Helmholtz, and convection-diffusion problems with different shaped domains. It is noted that in the 3D cases, the corresponding non-singular solutions have simpler forms, namely,

$$w_3^{\#}(r) = \frac{\sin(\lambda r)}{r} \tag{24}$$

for the Helmholtz,

$$u_3^{\#}(r) = \frac{\sinh(\lambda r)}{r} \tag{25}$$

for the modified Helmholtz, where sinh denotes the hyperbolic function, and

$$p_3^{\#}(r) = e^{-\frac{v \cdot r}{2D}} \frac{\sinh(\mu r)}{r} \tag{26}$$

for convection-diffusion, where μ is defined in Eq. (23).

It is stressed here that by using computer algebra package "Maple", we have verified that all the above RBF non-singular general solutions rigorously satisfy the corresponding homogeneous equations. Moreover, these general solutions are C^{∞} smoothness.

3. Results and discussions

To show the convergence, accuracy and stability of the BKM, we analysed a number of homogeneous Helmholtz, modified Helmholtz, and convection-diffusion problems with different 2D domain geometries shown in Figs. 1-3 and a 3D sphere. The average relative error in the following figures is defined as

$$err = \frac{1}{N}\sum_{k=1}^{N}\left|\frac{u_k - \overline{u}_k}{u_k}\right|, \tag{27}$$

where k is the index of inner nodes; u_k and $\overline{u}_k$ are respectively analytical and BKM solutions at inner node k; and N represents the number of interior nodes of interest. The interior knots were randomly chosen and shown as small crosses in Figs. 1-3 for the 2D cases. The blank circles along boundary represent the boundary knots. The convergence behaviour of the BKM is clearly shown in the given curves of the average relative error against knot numbers.

Case 1. 2D Helmholtz problems

The Helmholtz equation is fundamentally important in many engineering and science branches. Figs. 4 and 5 illustrate the average relative error curves for a Dirichlet homogeneous Helmholtz problem with the analytical solution

$$u(x, y) = \sin(x)\cos(y). \tag{28}$$

The domain geometries are ellipse, square, and square with an elliptical hole. The wave number of the non-singular general solution (20) is $\lambda=\sqrt{2}$ for this case. It is seen from both Figs. 4 and 5 that the BKM solutions consistently converge very quickly. For example, the convergence rate for the square plate is 31.8 before reaching the minimum relative error value. Fig. 6 displays the average relative error curve of the homogeneous Neumann Helmholtz problem with the same analytical solution and square domain shown in Fig. 1. It is observed that like the Dirichlet cases, the convergence behaviour of the Neumann problem is very sound and stable with a convergence rate of 50.7. After reaching the minimum values, the error curves have the oscillations of small range in all these cases. Numerically, one concludes that the BKM has the super-convergent speed in the present cases.

To investigate the Helmholtz problems with the medium and high wave numbers, consider the Dirichlet problem with analytical solution

$$u(x,y)=\sin(\lambda x)+\cos(\lambda y). \tag{29}$$

Figs. 7 and 8 respectively show the error curves for the cases involving wave number λ=20 and λ=100. It is found that in each figure, the BKM requires more knots to produce the solution of acceptable accuracy for the case with ellipse domain than for that with square domain. By comparing the results of Figs. 7 and 8, it is also noted that the higher the wave number, the more knots are necessary to suffice accuracy. The convergence curves of both cases are also quite oscillatory and show that the severe ill-conditioning seriously affects the solution accuracy.

To clearly expose the wave property of the Helmholtz problem, Fig. 9 illustrates the solution surface with wave number λ=20 in a square domain. Figs. 10 and 11 present the relative error surfaces using 12 and 18 BKM boundary knots, respectively, which were generated with the relative errors at 101×101 knots uniformly covering the unit square. It is seen that with the exception of the relatively less accurate solutions at very few knots, the BKM solution accuracy as a whole is quite high even with 12 boundary knots.

Case 2. 2D modified Helmholtz problems

The BKM is tested to the modified Helmholtz problems with analytical solution

$$u(x,y)=e^{x+y}. \tag{30}$$

λ in the corresponding non-singular general solution (13) is here equivalent to $\sqrt{2}$.

As a matter of interest, Fig. 12 shows the accurate solution surface of this Dirichlet problem with square domain. Figs. 13 and 14 display the corresponding relative error surfaces using the BKM with 8 and 20 boundary knots, respectively, where the error surfaces were also yielded by relative errors at 101×101 knots uniformly covering the unit square. It is surprising to note that the error surface of the 8 boundary knots BKM

is very smooth and regular, while, in contrast, that of BKM using 20 boundary knots is very random. In both cases, highly accurate solutions were obtained.

The relative error behaviours against the knot numbers are clearly illustrated in Figs. 5, 6 and 15, respectively. It is seen from Fig. 15 that the BKM converges stably and quickly in both Dirichlet cases involving ellipse and square domains. Furthermore, Fig. 5 shows that the BKM performs equally well for the Neumann case, while Fig. 6 demonstrates that the BKM is robust and yields very accurate solutions for the Dirichlet modified Helmholtz problem with relatively complex-shaped domain, a square with an elliptical hole.

Case 3. 2D convection-diffusion problems

Next, we look into the BKM solution of the steady Dirichlet convection-diffusion problems with analytical solution

$$u(x,y) = e^{-x} + e^{-y}. \tag{31}$$

The parameter μ in the non-singular general solution (22) is $\sqrt{2}/2$ for this case. The BKM average relative error curves are given respectively in Fig. 5 for square domain with an elliptical hole and Fig. 16 for both square and elliptical domains. It is seen from Fig. 16 that the BKM performs better in square domain case than in elliptical domain case. In the latter, the visible oscillation is observed for the larger numbers of knots. It is, however, worth stressing that the BKM solutions in both cases are very accurate. For the case involving square domain with elliptical hole, the BKM solution converges very quickly as shown in Fig. 5. From the above experiments, the boundary geometry seems not to have strong affect on the convergence and accuracy of the BKM solution.

Case 4. 3D Helmholtz, modified Helmholtz, and convection-diffusion problems

Finally, we examine the 3D Dirichlet problems under unit sphere domain. The analytical solutions are respectively

$$u(x,y,z)=\sin(x)\cos(y)\cos(z) \tag{32}$$

for the Helmholtz equation,

$$u(x,y,z)=e^{x}+e^{y}+e^{z} \tag{33}$$

for the modified Helmholtz equation, and

$$u(x,y,z)=e^{-x}+e^{-y}+e^{-z} \tag{34}$$

for the convection-diffusion equation. The characteristic parameters λ and μ in the corresponding non-singular solutions (13), (20) and (22) are $\sqrt{3}$, $\sqrt{3}$, and $\sqrt{3}/2$, respectively. The same Helmholtz and convection-diffusion cases involving a unit cube have been investigated in [33]. Here they are reanalysed to show the convergence and stability of the BKM through the curves of the relative errors against knot numbers. The average relative error curves of the BKM solutions at the interior knots of x=0,0.2,-0.4,0.5,-0.6,0.8,-0.9, y=z=0 are plotted in Fig. 17. It is noted that the BKM boundary knots on the sphere surface were taken randomly.

It is found that the accuracy of all three cases is constantly improved as the incremental BKM boundary knots. It is especially stressed that the programming effort for 2D and 3D cases makes no difference for the BKM. The present 3D experiments further confirm the excellent accuracy and efficiency of the BKM.

4. Concluding remarks

It is revealed from the forgoing relative error curve figures that with the increasing number of sampling BKM boundary nodes, the calculated results do exhibit convergence trend in all tested cases. Moreover, the convergence is quick and stable in general. The efficacy of the BKM formulation is validated for the Helmholtz,

modified Helmholtz, and convection-diffusion problems, which are practically important in a broad range of physical and engineering areas.

The present study was undertaken to numerically examine the convergence behaviour of the BKM. The given experiments meet this objective. The BKM has neither singular integration, slow convergence and mesh in the DR-BEM nor artificial boundary outside physical domain in the MFS. These merits lead to excellent performances in computational accuracy, efficiency and stability as shown in the preceding section 3. On the other hand, the method is extremely simple to learn and easy to program, especially for complicated shapes and higher dimensions. In shark contrast, the MFS suffers a severe difficulty in handling complex geometry problems [7,37] due to a controversial artificial boundary.

More theoretical analysis and experimental studies of the BKM should be beneficial. For example, we do not know by now if the BKM can be applied to exterior problems. We also do not have a mathematical proof of the solvability and convergence of the method although it always succeeds in various experiments. Some issues concerning the optimal location of the knots and the choice of the radial basis function in the context of the BKM for the inhomogeneous problem has yet to be investigated. This is the subject of the future study.

Acknowledgements

The work described in this paper was partially supported by a grant from the Research Grants Council of the Hong Kong Special Administrative Region, China (Project No. CityU 1178/02P). The first author was then a visiting research fellow to the Mathematics Department of City University of Hong Kong.

References

1. D. Nardini, C.A. Brebbia, A new approach to free vibration analysis using boundary elements. *Appl. Math. Modeling*, 7 (1983) 157-162.

2. P.W. Partridge, C.A. Brebbia, L.W. Wrobel, *The Dual Reciprocity Boundary Element Method*, Comput. Mech. Publ., Southampton, UK, 1992.
3. T. Yamada, L.C. Wrobel, H. Power, On the convergence of the dual reciprocity boundary element method, *Eng. Anal. BEM*, 13 (1994) 291-298.
4. M.A. Golberg, C.S. Chen, The method of fundamental solutions for potential, Helmholtz and diffusion problems. In *Boundary Integral Methods - Numerical and Mathematical Aspects,* ed. M.A. Golberg, pp. 103-176, Comp. Mech. Publ., 1998.
5. A. Bogomolny, Fundamental solutions method for elliptic boundary value problems, *SIAM J. Numer. Anal.* 22(4) (1985) 644-669.
6. J. Li, Mathematical justification for RBF-MFS**,** *Engng. Anal. Bound*. 25(10) (2001) 897-901.
7. J.H. Kane, *Boundary Element Analysis in Engineering Continuum Mechanics*, Prentice Hall, New Jersey, 1994.
8. K. Balakrishnan, P.A. Ramachandrant, A particular solution Trefftz method for non-linear Poisson problems in heat and mass transfer, *J. Comput. Phy.* 150 (1999) 239-267.
9. P.W. Partridge, B. Sensale, The method of fundamental solutions with dual reciprocity for diffusion and diffusion-convection using subdomains, *Eng. Anal. BEM*, 24 (2000) 633-641.
10. T. Kitagawa, Asymptotic stability of the fundamental solution method. *J. Comput. Appl. Math.* 38 (1991) 263-269.
11. W. Chen, M. Tanaka, New insights in boundary-only and domain-type RBF methods, *Int. J. Nonlinear Sci. Numer. Simulation*, 1(3) (2000) 145-152.
12. W. Chen, M. Tanaka, A meshfree, integration-free, and boundary-only RBF technique, *Comput. Math. Appls.* 43 (2002) 379-391.
13. P. Mendonca, C. Barcellos, A. Durate, Investigations on the hp-Cloud method by solving Timoshenko beam problems, *Comput. Mech*. 25 (2000) 286-295.
14. S. W. Kang, J. M. Lee, Y. J. Kang, Vibration analysis of arbitrarily shaped membranes using non-dimensional dynamic influence function, *J. Sound Vibr.*, 221(1) (1999) 117-132.
15. S. W. Kang, J. M. Lee, Eigenmode analysis of arbitrarily shaped two-dimensional cavities by the method of point-matching, *J. Acoust. Soc. Am.*, 107(3) (2000) 1153-1160.

16. S. W. Kang, J. M. Lee, Free vibration analysis of arbitrarily shaped plates with clamped edges using wave-type functions, *J. Sound Vibr*. 242(1) (2001), 9-26.
17. J. T. Chen, M. H. Chang, K. H. Chen, S. R. Lin, The boundary collocation method with meshless concept for acoustic eigenanalysis of two-dimensional cavities using radial basis function, *J. Sound Vibr*., 257(4) (2002), 667-711.
18. J. T. Chen, I. L. Chen, K. H. Chen, Y. T. Lee, Comments on "Free vibration analysis of arbitrarily shaped plates with clamped edges using wave-type function", *Comput. Mech.*, (in press), 2002.
19. J. T. Chen, M. H. Chang, I. L. Chung, Y. C. Cheng, Comment on "Eigenmode analysis of arbitrarily shaped two-dimensional cavities by the method of point matching", *J. Acoust. Sco. Am*. 111(1) (2002), 33-36.
20. J. T. Chen, M. H. Chang, K. H. Chen, I. L. Chen, Boundary collocation method for acoustic eigenanalysis of three-dimensional cavities using radial basis function, *Comput. Mech*., 29 (2002), 392-408.
21. G. DE MEY, A simplified integral equation method for the calculation of the eigenvalues of Helmholtz equation, *J. Acoust. Soc. Am*., 11 (1977) 1340-1342.
22. W. Chen, Symmetric boundary knot method, *Engng. Anal. Bound. Elem.,* 26(6) (2002) 489-494.
23. R.L. Hardy, Multiquadratic equations for topography and other irregular surfaces, *J. Geophys. Res*. 176 (1971**)** 1905-1915.
24. M. Powell, Recent advances in Cambridge on radial basis functions. *The 2nd International Dortmunt Meeting on Approximation Theory*, 1998.
25. R. Schaback, H. Wendland, Numerical techniques based on radial basis functions. In *Curve and Surface Fitting*: Saint-Malo 1999, ed. A. Cohen et al., pp. 359-374, Vanderbilt University Press, 2000.
26. E.J. Kansa, Multiquadrics: A scattered data approximation scheme with applications to computational fluid dynamics. *Comput. Math. Appl*. 19 (1990) 147-161.
27. X. Zhang X.H. Liu, K.Z. Song, M.W. Lu, Least-square collocation meshless method, *Int. J. Numer. Methds. Engng.,* 51(9) (2001) 1089-1100.
28. X. Zhang, M.W. Lu, J.L. Wegner, A 2-D meshless model for jointed rock structures, *Int. J. Numer. Methds. Engng.* 47(10) (2000) 1649-1661.
29. X. Zhang, K.Z. Song, M.W. Lu, Meshless Methods Based on Collocation with Radial Basis Functions, *Comput. Mech.* 26(4) (2000) 333-343.

30. Y.C. Hon, X.Z. Mao, A radial basis function method for solving options pricing model. *Financial Eng.* 81(1) (1999) 31-49.
31. W. Chen, M. Tanaka, Relationship between boundary integral equation and radial basis function, in *The 52th Symposium of JSCME on BEM*, ed. M. Tanaka, Tokyo, 2000.
32. W. Chen, W. He, A note on radial basis function computing, *Int. J. Nonlinear Modelling Sci. Eng*., 1 (2001) 59-65.
33. Y.C. Hon, W. Chen, Boundary knot method for 2D and 3D Helmholtz and convection-diffusion problems with complicated geometry, (in press), 2002.
34. M. Golberg, C.S. Chen, H. Bowman, H. Power, Some comments on the use of radial basis functions in the dual reciprocity method, *Comput. Mech.* 21 (1998) 141-148.
35. M. Zerroukat, H. Power, C.S. Chen, A numerical method for heat transfer problems using collocation and radial basis function, *Int. J. Numer. Method Eng*. 42 (1998) 1263-1278.
36. H. Ding, C. Shu, K.S. Yeo, Simulation of natural convection in an eccentric annulus between a square outer cylinder and a circular inner cylinder using the local MQ-DQ method, (submitted), 2002.
37. K. Balakrishnan, P.A. Ramachandran, The method of fundamental solutions for linear diffusion-reaction equations, *Math. Comput. Modelling.* 31 (2000) 221-237.

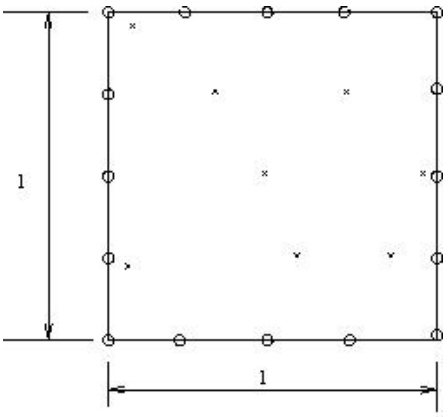

Fig. 1. Configuration of a square domain

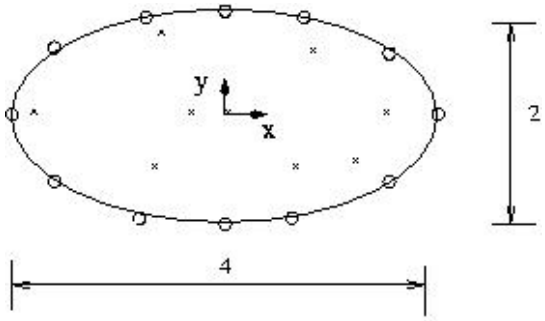

Fig. 2. Configuration of an ellipse

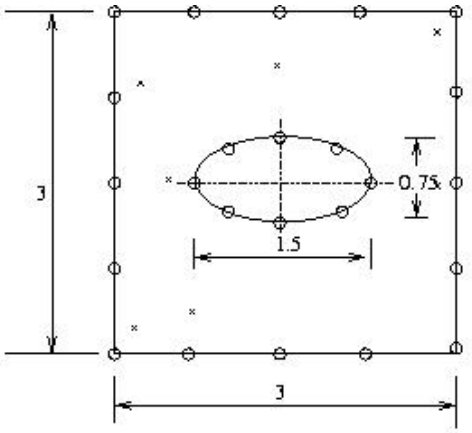

Fig. 3. Configuration of a square with an elliptical hole

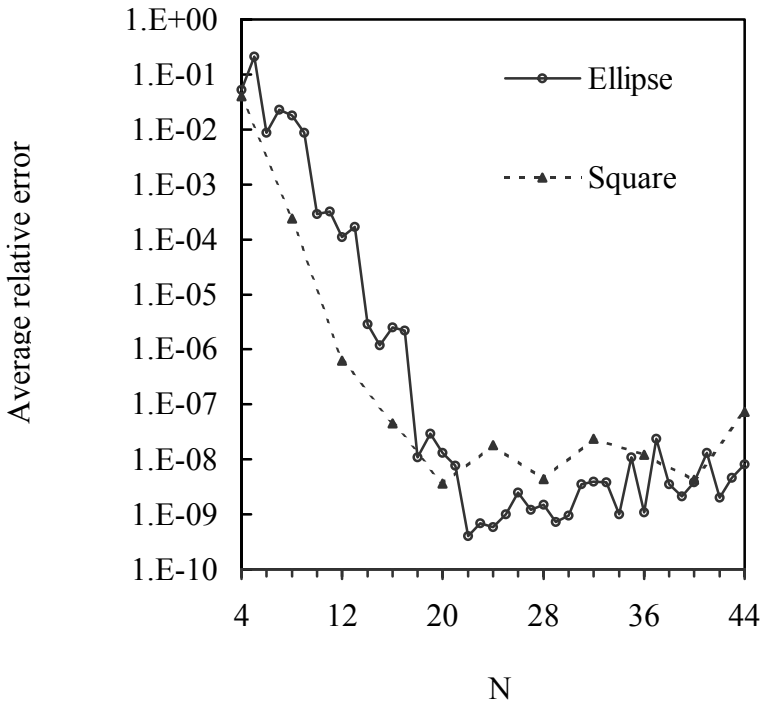

Fig. 4. Average relative error curves for Dirichlet Helmholtz problems with elliptical and square domains

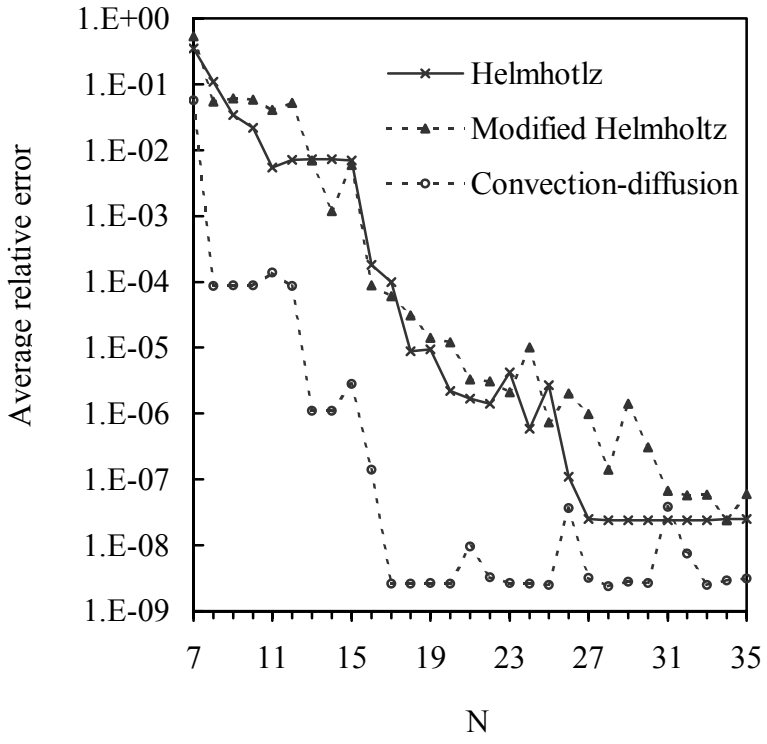

Fig. 5. Average relative error curves for Dirichlet Helmholtz, modified Helmholtz, and convection-diffusion problems with square domain with elliptical hole

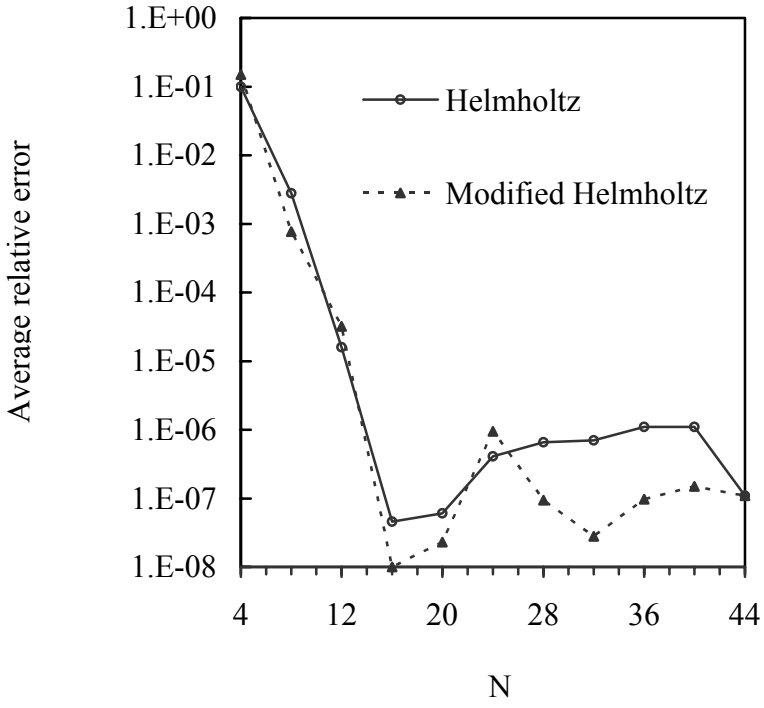

Fig. 6. Average relative error curves for Neumann Helmholtz and modified Helmholtz problems with square domain

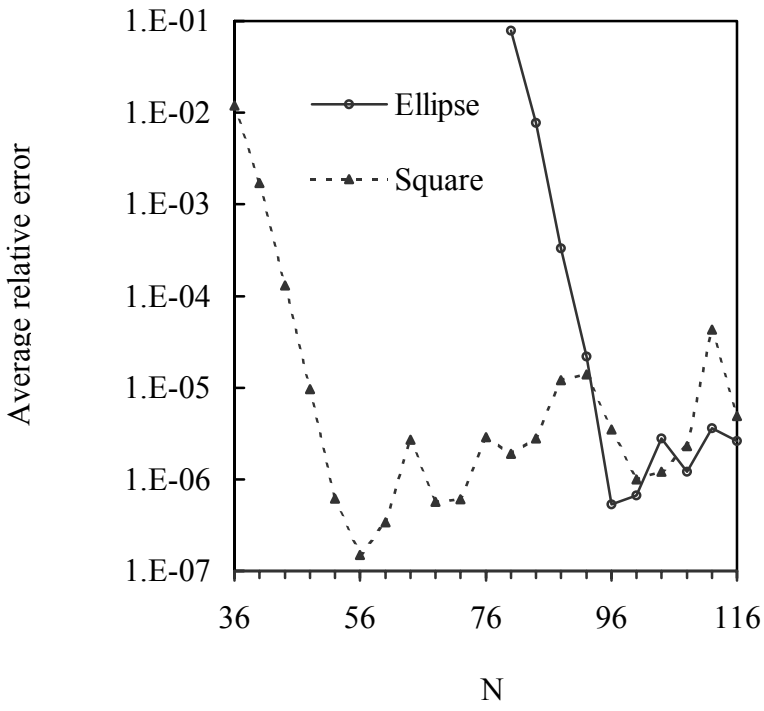

Fig. 7. Average relative error curves for Dirichlet Helmholtz problems with medium wave number λ=20

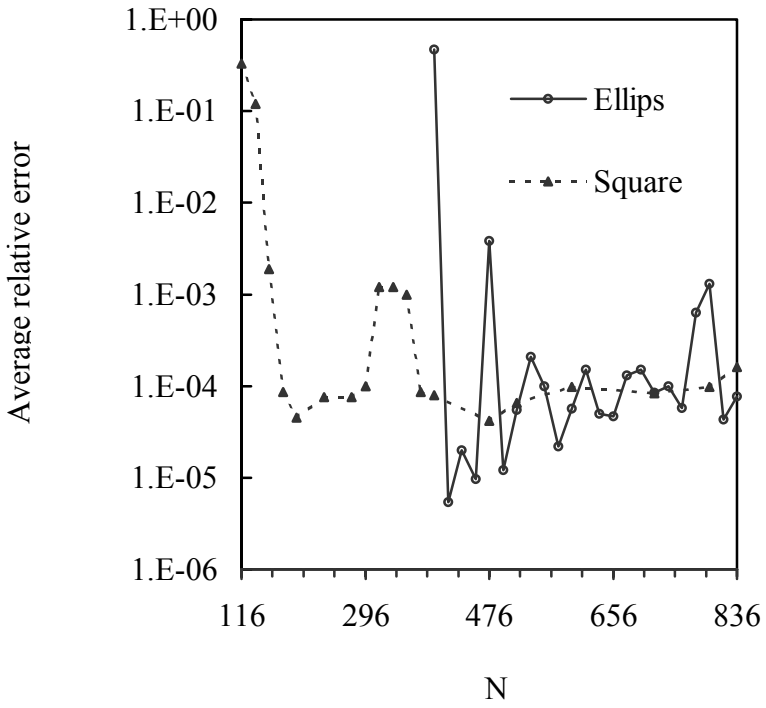

Fig. 8. Average relative error curves for Dirichlet Helmholtz problems with high wave number λ=100

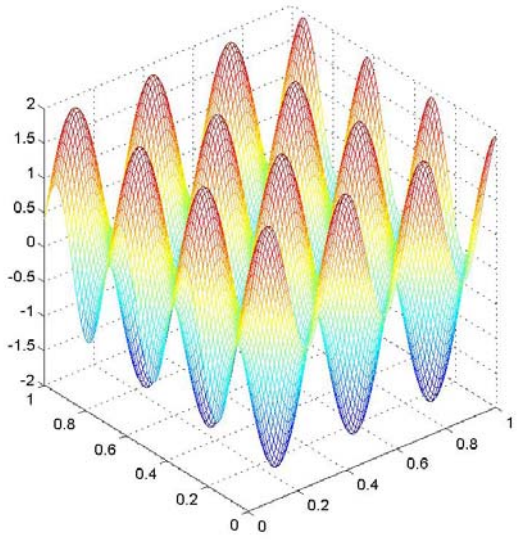

Fig. 9. Wave profile of Dirichlet Helmholtz problem of wave number 20

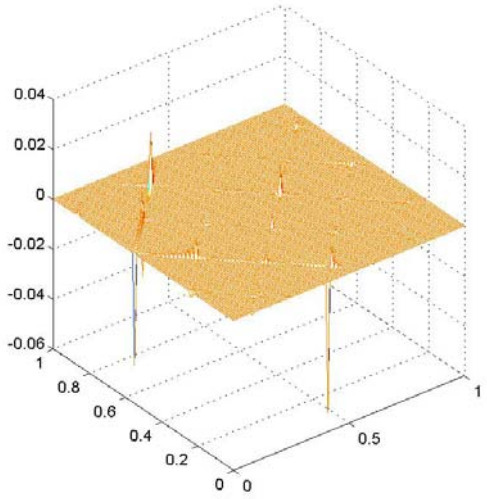

Fig. 10. Relative error surface of Dirichlet Helmholtz problem of wave number 20 using 12 BKM boundary knots

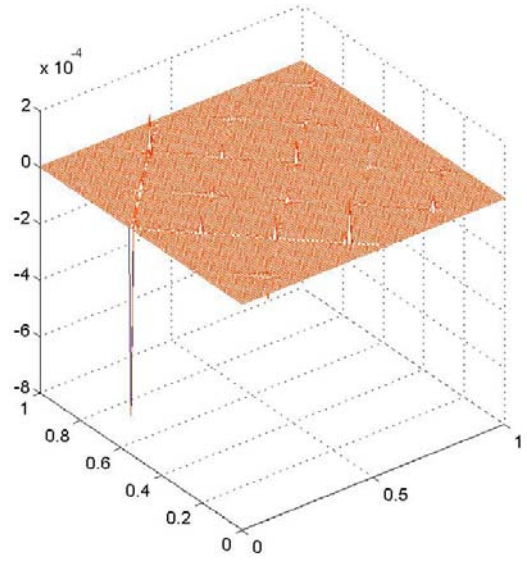

Fig. 11. Relative error surface of Dirichlet Helmholtz problem of wave number 20 using 18 BKM boundary knots

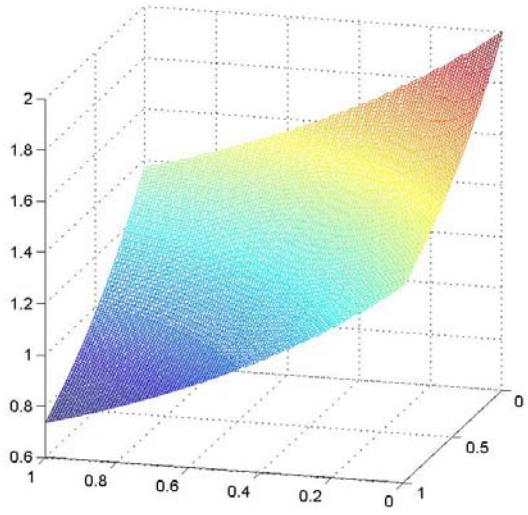

Fig. 12. Solution profile of Dirichlet modified Helmholtz problem

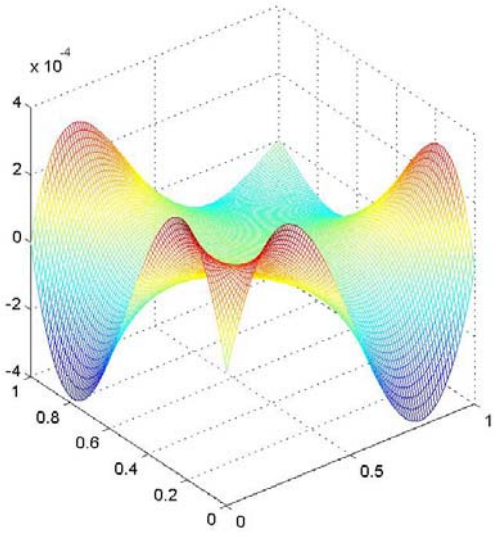

Fig. 13. Relative error surface of Dirichlet modified Helmholtz problem of wave number 20 using 8 BKM boundary knots

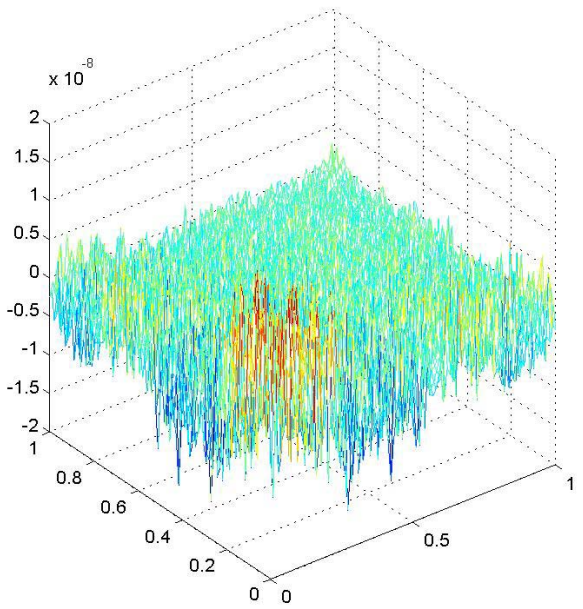

Fig. 14. Relative error surface of Dirichlet modified Helmholtz problem of wave number 20 using 20 BKM boundary knots

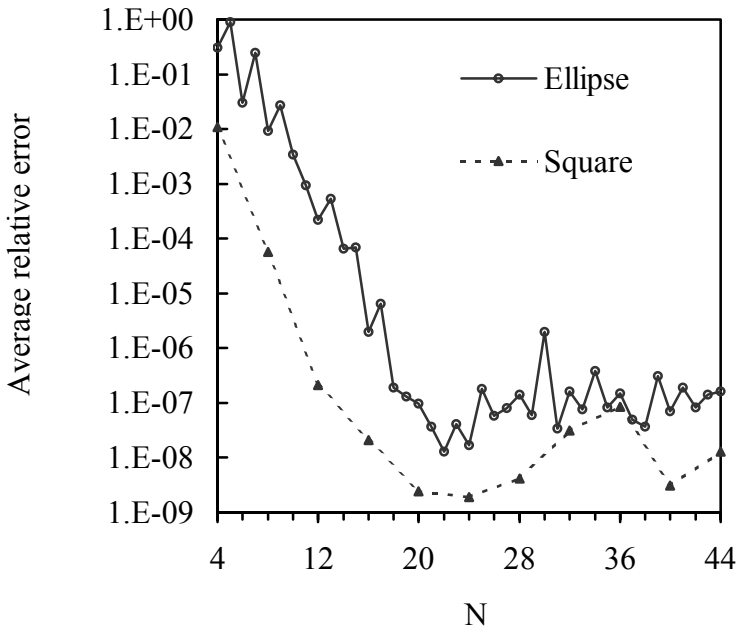

Fig. 15. Average relative error curves for Dirichlet modified Helmholtz problem with elliptical and square domains

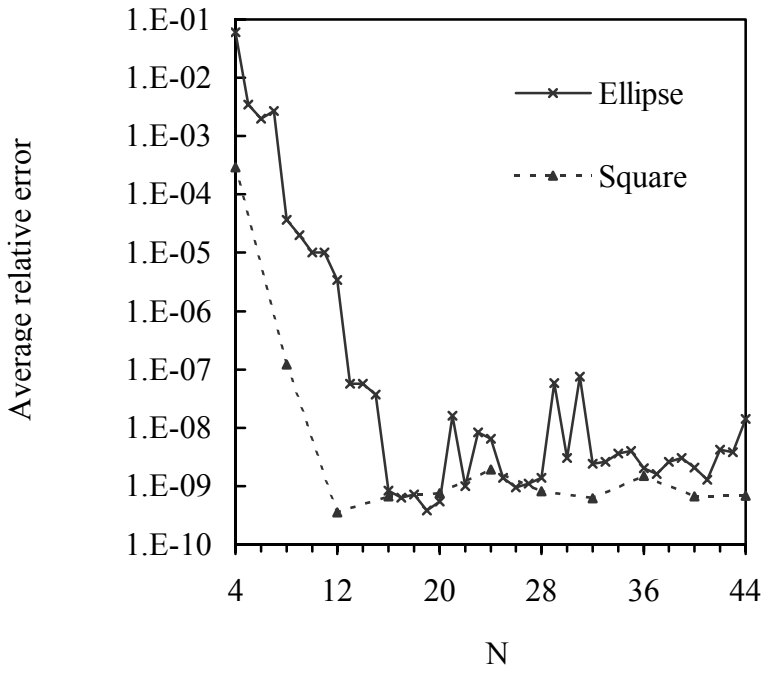

Fig. 16. Average relative error curves for Dirichlet convection-diffusion problem with elliptical and square domains

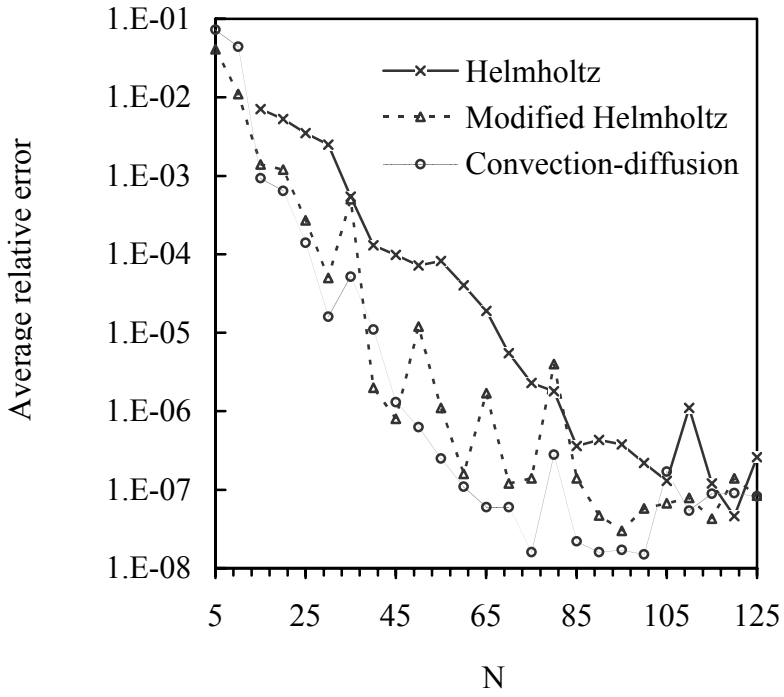

Fig. 17. Average relative error curve for Dirichlet Helmholtz, modified Helmholtz and convection-diffusion problems with 3D sphere domain